JHEP PROCEEDINGS

International Europhysics Conference on HEP

Recent Results from Super-Kamiokande

Shigetaka MORIYAMA* **on behalf of the Super-Kamiokande Collaboration**

Address: Kamioka Observatory, Institute for Cosmic Ray Research, University of Tokyo, Higashi-Mozumi, Kamioka, Gifu 506-1205, Japan
E-mail: moriyama@icrr.u-tokyo.ac.jp

ABSTRACT: Results from the atmospheric and solar neutrino analyses at Super-Kamiokande are presented. The whole data set of atmospheric neutrinos is consistently explained by the assumption of pure ν_μ-ν_τ oscillations. The allowed range of parameters is $1.7 \times 10^{-3} < \Delta m^2 < 3.8 \times 10^{-3}\,\mathrm{eV}^2$ and $\sin^2 2\theta > 0.90$ at 90% C.L. Since the smoking gun of ν_μ-ν_τ oscillations would be the observation of the τ appearance, we also searched for charged-current (CC) ν_τ events. We used three methods to enrich the CC ν_τ events and their results are consistent with the ν_τ appearance. From the solar neutrino data, we obtained the ^{8}B neutrino flux ratio to the prediction of the standard solar model to be $0.451 \pm 0.005 \pm^{0.016}_{0.014}$. The flux difference of daytime and nighttime is 1.3σ. The energy spectrum is consistent with expectations. By examining the daytime and nighttime spectra, we found the large mixing angle solutions, which satisfy the observed fluxes of the solar neutrino experiments, are favored for the ν_e-$\nu_{\mu,\tau}$ oscillations. On the other hand, the ν_e-ν_{sterile} oscillations are disfavored at 95% C.L. The oscillation analysis results including new SNO data are also reviewed.

PrHEP hep2001

1. Introduction

The Super-Kamiokande (SK) detector gives us a great opportunity to observe neutrino oscillations. The parent atmospheric neutrinos of the observed events have a wide range of energies, 100 MeV-100 GeV, and flight lengths, 10 km-13000 km. Combined with the ability to distinguish the flavors of parent neutrinos, this makes it possible to measure the neutrino oscillations with Δm^2 down to $10^{-4}\mathrm{eV}^2$. For the solar neutrinos, SK can give the energy spectrum of the recoil electrons as well as real time information of the events. These features are utilized to obtain flux-independent information on possible solar neutrino oscillations. In this presentation, the results of the atmospheric neutrino analysis and the solar neutrino analysis are reported.

*Speaker.

2. Atmospheric Neutrino

Primary cosmic rays interact with air nuclei and produce secondary mesons. The atmospheric neutrinos are decay products of these secondaries. The flavor ratio of the flux $\frac{\nu_\mu+\bar{\nu}_\mu}{\nu_e+\bar{\nu}_e}$ has been calculated with an accuracy better than 5%. For the neutrino energies greater than a few GeV, the zenith angle distribution of the flux is expected to be up-down symmetric.

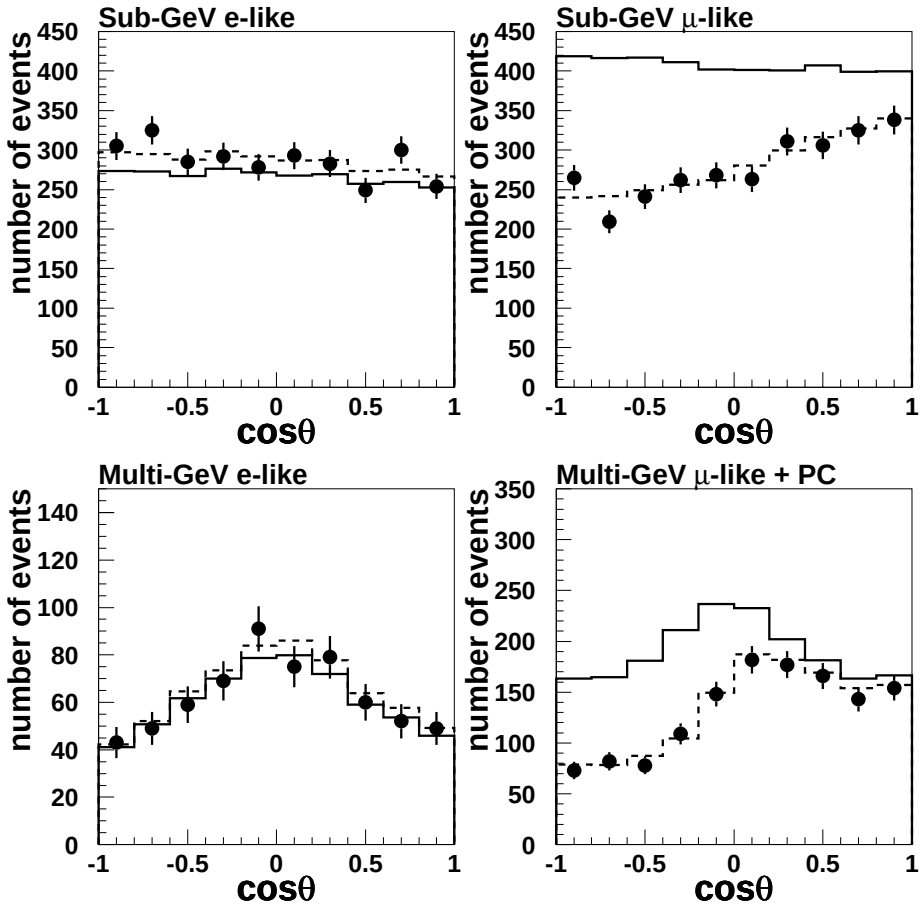

Figure 1: Zenith angle distributions of Sub-GeV and Multi-GeV samples. The solid histograms show the MC prediction without oscillation and the dashed histograms show the MC prediction for the ν_μ-ν_τ oscillations with $\sin^2 2\theta = 1.0$ and $\Delta m^2 = 2.5 \times 10^{-3}\mathrm{eV}^2$

Neutrino events produced in the inner detector are categorized as fully-contained (FC) and partially-contained (PC) events according to the amount of the outer detector activity. FC events are subdivided into Sub-GeV ($E_{\mathrm{vis.}} < 1.33\,\mathrm{GeV}$) and Multi-GeV ($E_{\mathrm{vis.}} > 1.33\,\mathrm{GeV}$) samples according to the amount of visible energy. Events with only one reconstructed ring are subdivided into e-like and μ-like based on the likelihood analysis of the detected Cherenkov ring pattern. Multi-ring events are also identified as e-like or μ-like based on the Cherenkov ring pattern of the most energetic rings. The flavor ratio is evaluated by the ratio between the data and expectation without oscillations:

PrHEP hep2001

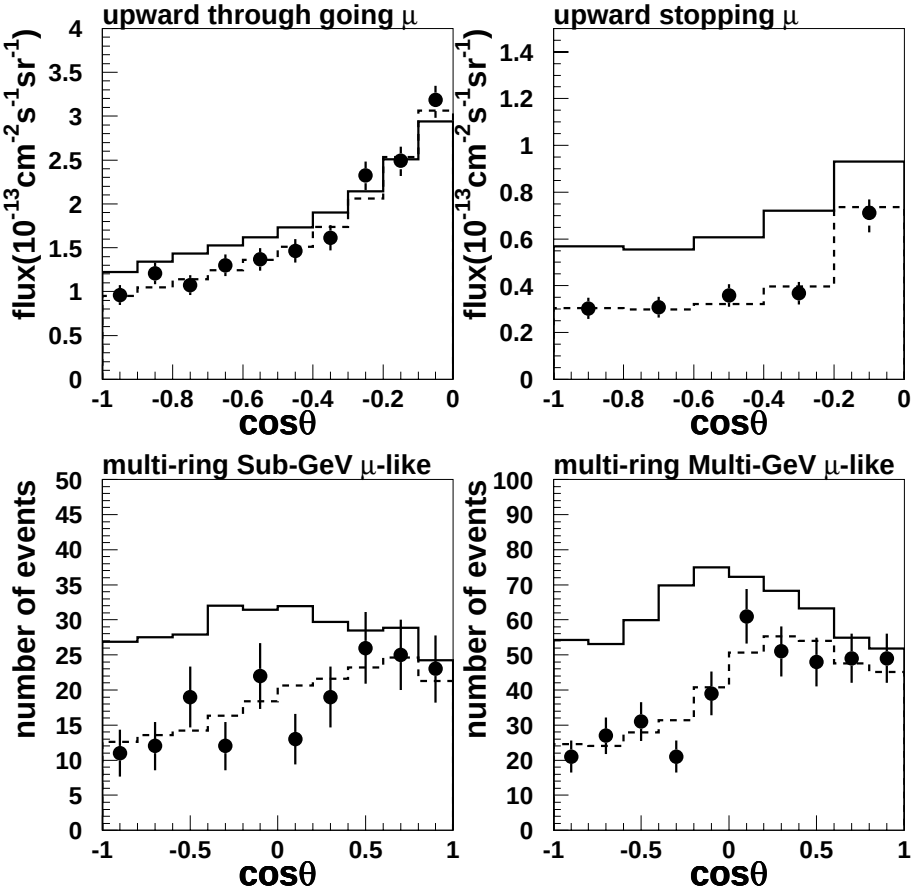

Figure 2: Zenith angle distributions of upward going muons and multi-ring samples. The solid histograms show the MC prediction without oscillation and the dashed histograms show the MC prediction for ν_μ-ν_τ oscillations with $\sin^2 2\theta = 1.0$ and $\Delta m^2 = 2.5 \times 10^{-3}\mathrm{eV}^2$

$R = \frac{(\mu\text{-like}/e\text{-like})_{\mathrm{Data}}}{(\mu\text{-like}/e\text{-like})_{\mathrm{MC}}}$. "Upward-going muons" is another category of neutrino events. They are entering muons produced by neutrinos in the rock surrounding the SK detector. They are subdivided into "upward-through" muons and "upward-stopping" muons depending on whether the muons penetrate the SK detector or stop in it.

The analysis shown here is based on a 1289-day data sample for the FC and PC samples, 1268-day data for the upward-stopping muons, and 1248-day data for the upward-through muons. The zenith angle distributions are shown in Fig. 1 and Fig. 2. The measured R values for the Sub-GeV and Multi-GeV data are $0.638 \pm 0.017 \pm 0.050$ and $0.675^{+0.034}_{-0.032} \pm 0.080$, respectively. The up-down asymmetry of the zenith angle distributions and the small R values indicate neutrino oscillations.

2.1 Two flavor ν_μ-ν_τ oscillation analysis

The FC, PC, and upward going muon samples are employed to obtain the allowed regions for the neutrino oscillation parameters, which are shown in Fig. 3. The minimum χ^2 is found to be 157.5/170 d.o.f. at $\sin^2 2\theta = 1.00$ and $\Delta m^2 = 2.5 \times 10^{-3}\mathrm{eV}^2$, whereas χ^2 for no

PrHEP hep2001

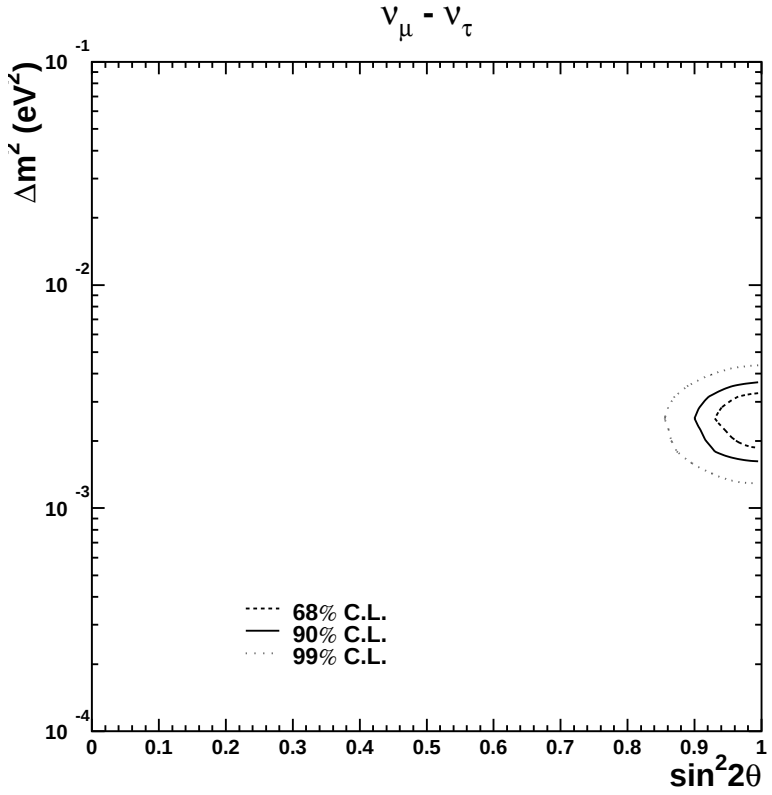

Figure 3: Allowed neutrino oscillation parameter regions obtained by Sub-GeV+Multi-GeV+PC+upward-going muons+multi-ring samples.

oscillations is 393.4/172 d.o.f. The dotted histograms in Fig. 1 and Fig. 2 show the zenith angle distributions with the best fit parameters.

2.2 Search for charged current ν_τ events

The evidence for atmospheric neutrino oscillation is based on the disappearance of ν_μ events. It imposes on us the task of discriminating the oscillation partners of ν_μ. There are two kinds of possible scenarios: ν_μ-ν_τ or ν_μ-$\nu_{\rm sterile}$. As for the ν_μ-$\nu_{\rm sterile}$ oscillation case, we have excluded the pure ν_μ-$\nu_{\rm sterile}$ oscillation scenario at 99% C.L. as an explanation of the atmospheric neutrino oscillation [1]. In this talk, we will report on the analyses of the ν_τ appearance.

The observation of ν_τ appearance is difficult because

- τ events mainly decay immediately to hadrons. Since ν_e or ν_μ can produce hadrons via neutral current, they mimic the τ events. A water Cherenkov detector with finite resolution like SK does not have a high discrimination power.

- A charged current (CC) interaction would produce the τ lepton only above 3.4 GeV of neutrino energy. If we assume $\sin^2 2\theta = 1$ and $\Delta m^2 = 3.0 \times 10^{-3}\mathrm{eV}^2$, the τ event rate is only 20 events/year.

PrHEP hep2001

However, we can enrich the CC ν_τ events based on differences between the CC ν_τ events and background. First of all, we applied the primary cut for the CC ν_τ events: (1) fully contained, (2) multi-GeV ($E_{vis} > 1.33\,\mathrm{GeV}$), and (3) the most energetic ring is e-like. The signal to background ratio after this cut is found to be 3.5% based on the Monte Calro study. After this primary cut, we tried the following three methods:

1. Likelihood analysis using standard SK variables, i.e., visible energy, number of rings, number of decay electrons, and so on.
2. Neural network method using standard SK variables.
3. Likelihood method using energy flow and event shape.

Here, the first method is explained in detail.

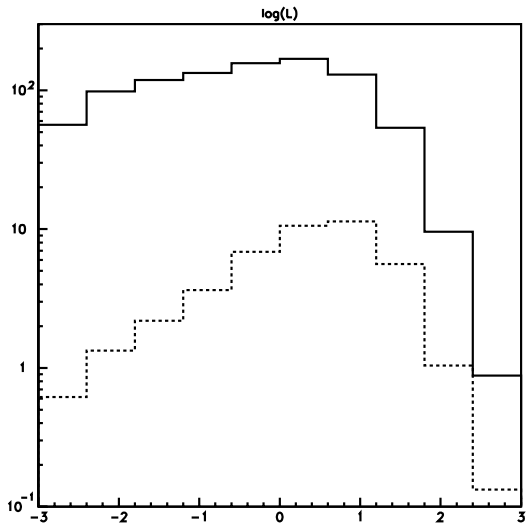

Figure 4: Likelihood distributions for multi-ring event, Monte Carlo samples. The solid line shows the likelihood distribution for background. The dashed line shows the likelihood distribution for the CC ν_τ events. The horizontal axis is $\log(\mathcal{L}_{\mathrm{total}})$. They are normalized by live time.

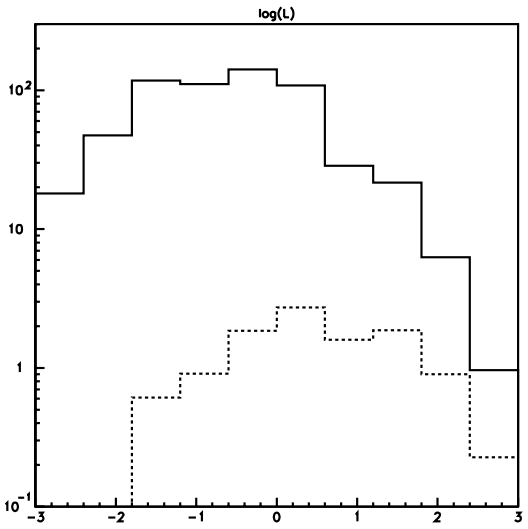

Figure 5: Likelihood distributions for single-ring event, Monte Carlo samples. The solid line shows the likelihood distribution for background. The dashed line shows the likelihood distribution for the CC ν_τ events. The horizontal axis is $\log(\mathcal{L}_{\mathrm{total}})$. They are normalized by live time.

When we construct the likelihood using several SK variables, they were carefully selected to maximize the differences between the signal and background, and to reduce the systematic errors. We used Monte Calro samples with an assumption of $\sin^2 2\theta = 1$, $\Delta m^2 = 3.0 \times 10^{-3}\mathrm{eV}^2$, and defined the tau likelihood as $\mathcal{L}_{\mathrm{total}}$. Since some of the variables are defined only for multi ring events, we treated the multi-ring events and single-ring events separately. Fig. 4 and Fig. 5 show the likelihood distribution after the primary cut for the multi-ring events and for single-ring events, respectively. We set the cut position

PrHEP hep2001

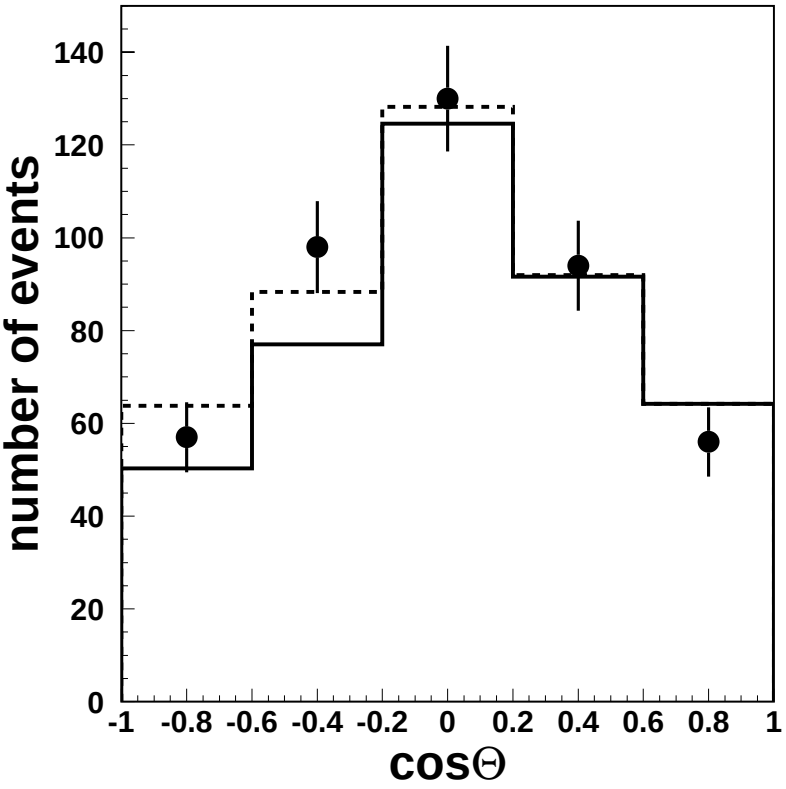

Figure 6: Zenith angle distribution after likelihood cut. Dots represent data. The solid histogram and dotted histogram show the background and signal, respectively. The histograms show the best fit for the zenith fitting with data. See text for details.

at $\log(\mathcal{L}_{\rm total}) = 0$ and 1 for each data set to maximize the significances. By using the likelihood cut, the signal to background ratio is increased from 4.6% to 8% for multi-ring events, and from 1.8% to 8% for single-ring events. We checked the likelihood distributions by only using the Monte Carlo samples and downward-going real data, in which ν_τ does not exist, to perform the blind analyses.

After we finished all the studies based on Monte Calro samples and downward-going real data, we opened the upward-going samples. Fig. 6 shows the zenith angle distribution of the final samples after the likelihood cut. We fitted the zenith angle distribution of data with a linear sum of the zenith shape of the background and signal. In this figure, the best fitted results are plotted. In the analysis, we minimized

$$\chi^2 = \sum_{\cos\Theta}^{5} \left(\frac{N_{data} - \left(\alpha N^{\tau}_{MC} + \beta N^{BG}_{MC}\right)}{\sigma} \right)^2 , \tag{2.1}$$

where N_{data} indicates the number of events in the zenith bin, N^{BG}_{MC} is the number of expected background events, and N^{τ}_{MC} is the number of expected signals. α and β are the fitting parameters. The Monte Carlo samples are normalized with live time. As the best fit, we obtained $\alpha = 0.90$ and $\beta = 1.02$ with $\chi^2_{min} = 2.91/3$. From this value, we obtained $N^{FC}_{\tau} = \alpha N^{\tau}_{obs}/\mathrm{eff} = 66 \pm 41(\mathrm{stat.})^{+25}_{-18}(\mathrm{sys.})$, which is the number of signals

PrHEP hep2001

in the fully contained samples. Since the expected value for N_τ^{FC} is 74, this value is consistent with the expected one. Two other analyses gave similar results. Analysis #2 gives $N_\tau^{FC} = 92 \pm 41^{+17}_{-23}$, and analysis #3 gives $N_\tau^{FC} = 79^{+44}_{-40}$. In conclusion, our data is consistent with tau appearance.

3. Solar Neutrino

The most plausible solution for the solar neutrino problem is the neutrino oscillations. Using the fluxes observed by solar neutrino experiments (Homestake, GALLEX, SAGE, and SK), there are four allowed regions: large mixing angle (LMA), small mixing angle (SMA), low (LOW), and vacuum oscillation (VO) regions. The most urgent task for the solar neutrino problem is to find a model independent evidence for the neutrino oscillations and pin down a single set of oscillation parameters. For this purpose, the zenith angle spectra explained below are quite important. The result presented here is described in detail in Ref. [2] and Ref. [3].

As presented at this conference [5], the SNO collaboration provided a new result for the measurement of the ^{8}B charged-current reaction rate [6]. Several authors already gave combined analyses [7]. Some comments will be given about the results.

3.1 Flux, Day/Night Flux, Energy Spectrum

We have obtained the total solar neutrino signal of $18{,}464 \pm 204 \pm^{646}_{554}$ events based on a 1258-day data sample. The resulting total ^{8}B solar neutrino flux is 2.32 ± 0.03(stat.) $\pm^{0.08}_{0.07}$ (sys.) $\times 10^6 \mathrm{cm}^{-2}\mathrm{s}^{-1}$. The ratio to the expected flux for the standard solar models (SSM, BP98) is 0.451 ± 0.05(stat.) $\pm^{0.016}_{0.014}$ (sys.).

Fig. 7 shows the day and night fluxes. The measured day and night fluxes corrected for the solar eccentricity of the earth's orbit at 1 AU are 2.28 ± 0.04(stat.) $\pm^{0.08}_{0.07}$ (sys.) $\times$ $10^6 \mathrm{cm}^{-2}\mathrm{s}^{-1}$ for the daytime and 2.36 ± 0.04(stat.) $\pm^{0.08}_{0.07}$ (sys.) $\times 10^6 \mathrm{cm}^{-2}\mathrm{s}^{-1}$ for the nighttime. The flux difference is $\frac{N-D}{(N+D)/2} = 0.033 \pm 0.022$(stat.) $\pm^{0.013}_{0.012}$ (sys.).

Fig. 8 shows the observed electron energy spectrum in the ratio to the expectation from the SSM. Since χ^2 for the flat is 19.0/18 d.o.f. (39% C.L.), we can exclude the oscillation parameters which predict a strong spectrum distortion.

3.2 Oscillation Analysis

We performed two kinds of oscillation analyses. One is a test which gives the exclusion area by using only the spectral shape information of SK. This means a flux-independent analysis based on only the SK data. This area can be compared with the allowed area obtained by using the flux information from all existing solar neutrino experiments. Another analysis gives allowed area, which is obtained by using both the flux information and spectral information of SK.

For the analyses, the sample is divided into seven zenith angle bins: one day bin and six bins in $\cos\theta_z$ for the night. For each zenith angle bin, the data are divided into eight recoil electron energy bins. We call this binning the "zenith angle spectrum." The definition of the binning can be found in Ref. [3].

PrHEP hep2001

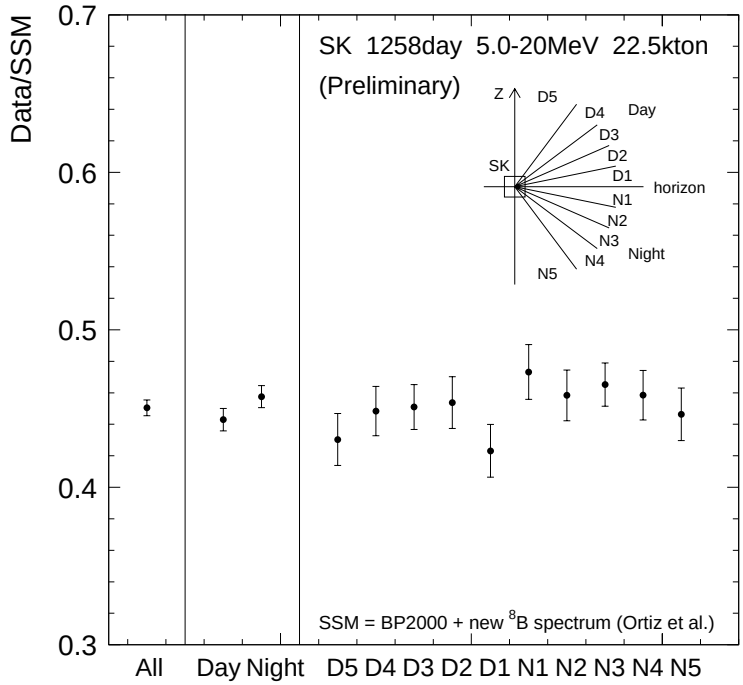

Figure 7: Solar neutrino flux as a function of the nadir of the sun. The day and night data are divided by an interval shown in the figure.

Figs. 9 and 10 show the results. See the caption for the definitions of area. From the figures, we can see that the SMA and VO solutions are disfavored for $\nu_e \leftrightarrow \nu_{\mu,\tau}$. Pure $\nu_e \leftrightarrow \nu_{\rm sterile}$ is also disfavored at 95% C.L. By using the SK data with a flux constraint, the large mixing solutions are favored.

3.3 Impact of SNO Result on Oscillation Analysis

The recent result from the SNO collaboration has a significant impact on the physics of solar neutrino oscillations. The significant difference between the CC event rate measured by SNO and the electron recoil event rate measured by SK means that the solar neutrinos oscillate. Several authors have already provided combined analyses [7] for the oscillation parameters. For example, Fogli and Lisi show allowed areas of solar neutrino oscillation parameters with and without new SNO results. The most important point is that the SMA solutions are strongly disfavored if we use all the available experimental data as shown in Fig. 7 in Ref. [7]. It is also interesting to compare Fig. 5 and Fig. 6 in the reference; the former figure is obtained without the SNO CC event rate and the latter figure is obtained without the SK daytime-nighttime spectral shape information. From the figures, one can see the importance of the SK spectral information as well as the SNO CC event rate measurement.

PrHEP hep2001

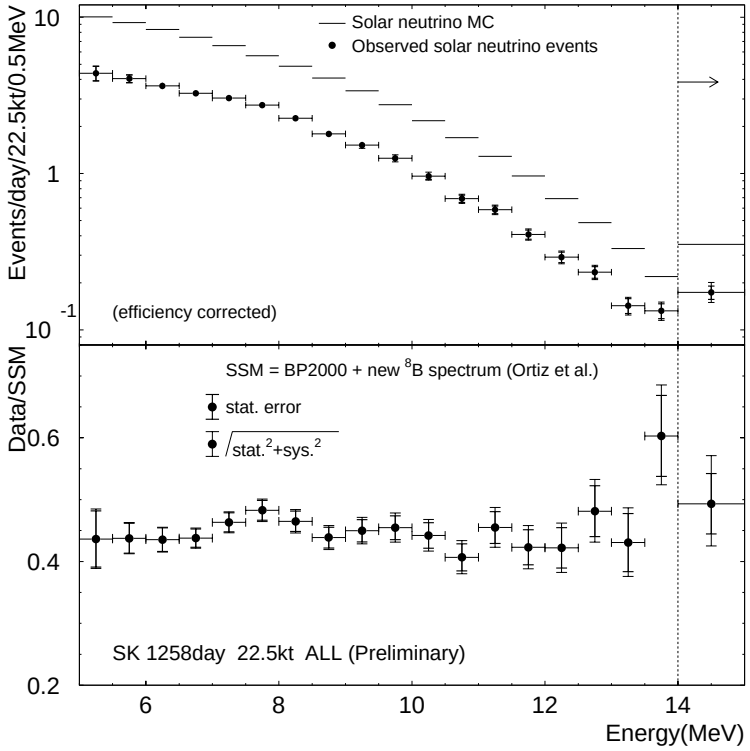

Figure 8: Energy spectrum of solar neutrinos. Upper figure shows data (dots), and predicted number of events based on SSM (lines). Bottom figure shows data/SSM as a function of energy. Although the observed event rate is much smaller than expected, the observed spectrum shape is consistent with the flat one.

4. Summary

We updated the flavor ratio and the zenith angle distribution of atmospheric neutrinos. For pure ν_μ-ν_τ oscillations, the allowed parameters are $1.7 \times 10^{-3} < \Delta m^2 < 3.8 \times 10^{-3}\,\text{eV}^2$ and $\sin^2 2\theta > 0.90$ at 90% C.L. We also searched for the charged-current ν_τ events and found that the number of events in the fully contained sample is $66 \pm 41(\text{stat.})^{+25}_{-18}(\text{sys.})$. This is consistent with the expected value for $N^{FC}_{\tau,\text{exp}} = 74$.

For the solar neutrinos, we updated the ^{8}B flux, the day and night fluxes, and energy spectrum of the solar neutrinos. The difference between the day and night fluxes is 1.3σ. The energy spectrum shape is consistent with the expectation. As an oscillation analysis, we obtained the 95% C.L. excluded regions. By examining the daytime and nighttime spectra, we found the large mixing angle solutions, which satisfy the observed fluxes of solar neutrino experiments, are favored for the ν_e-$\nu_{\mu,\tau}$ oscillations. On the other hand, the ν_e-ν_{sterile} oscillations are disfavored at a 95% C.L.

References

[1] S. Fukuda *et al.,* Phys. Rev. Lett. 85, 3999-4003 (2000).

[2] S. Fukuda *et al.,* Phys. Rev. Lett. 86, 5651 (2001).

PrHEP hep2001

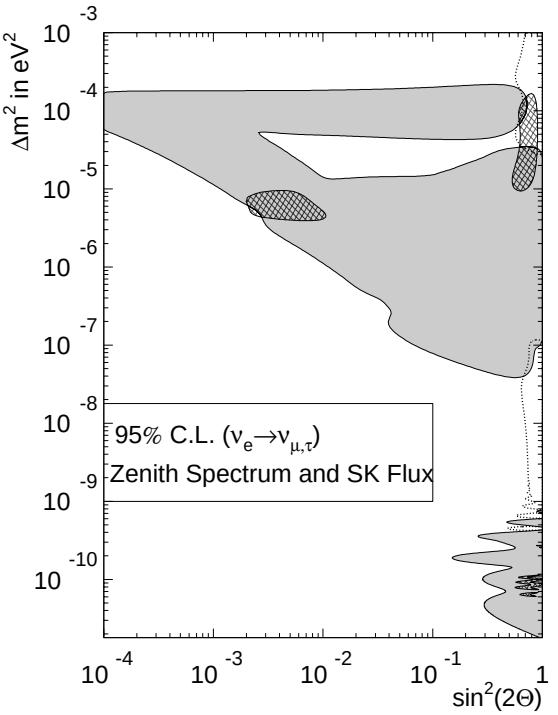

Figure 9: Exclusion area for two-flavor oscillation $\nu_e \leftrightarrow \nu_{\mu,\tau}$ from flux-independent zenith angle spectrum analysis (gray areas). The areas inside the dotted lines show the allowed areas obtained by the flux-constraint analysis using the zenith angle spectrum and the SSM flux prediction. The cross hatched areas are allowed in a combined fit based only on the absolute fluxes measured at GALLEX, SAGE, Homestake, and SK.

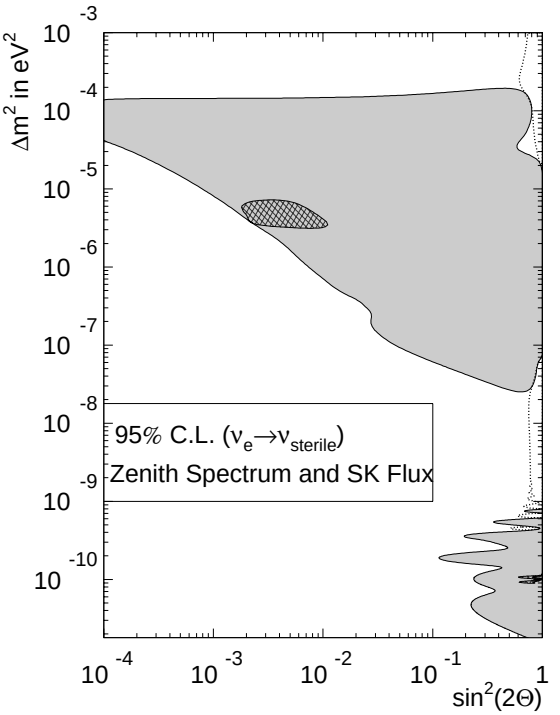

Figure 10: Exclusion and allowed areas for two-flavor oscillation $\nu_e \leftrightarrow \nu_{\rm sterile}$

PrHEP hep2001

[3] S. Fukuda *et al.,* Phys. Rev. Lett. 86, 5656 (2001).

[4] Y. Fukuda *et al.,* Phys. Rev. Lett. 85, 3999 (2000).

[5] A. McDonald, in these proceedings.

[6] Q. R. Ahmad *et al.,* Phys. Rev. Lett. 87, 071301 (2001).

[7] John N. Bahcall, M. C. Gonzalez-Garcia, Carlos Pena-Garay, hep-ph/0106258; G. L. Fogli, E. Lisi, hep-ph/0106247